Verification and validation of CgWind: a high-order accurate simulation tool for wind engineering

Kyle K. Chand[a] and Michael A. Singer[b]
[a]*Lawrence Livermore National Laboratory, Livermore, CA, USA, chand1@llnl.gov*
[b]*Lawrence Livermore National Laboratory, Livermore, CA, USA, singer3@llnl.gov*

ABSTRACT: This paper presents the verification and initial validation of CgWind, a new, high-fidelity, large eddy simulation code for wind engineering applications. CgWind utilizes fourth-order accurate spatial discretizations of the incompressible Navier-Stokes equations on composite, structured grids to achieve both high efficiency and high spatial resolution without sacrificing the ability to model complex and moving geometries. Computational models such as CgWind consist of complex numerical algorithms and software whose correctness must be verified prior to use as a mathematical model for practical simulations. The process of *verification* demonstrates that a numerical model is implemented correctly and confirms the theoretical properties (stability and accuracy) of the discrete approximations of the continuous mathematical model. After verified successfully, *validation* then determines the suitability of the mathematical model to capture the relevant physical phenomena for problems of interest. Rigorous verification has been built into the development of CgWind, and verification of accuracy and convergence has been demonstrated. The code is now undergoing validation by comparison to experimental data.

1 INTRODUCTION

CgWind is a new, high-fidelity simulation tool designed to meet the modeling requirements of advanced wind engineering applications. The tool couples large eddy simulation (LES) models, based on the incompressible Navier-Stokes equations, with moving grid techniques designed to resolve flow near bodies in relative motion such as turbine blades (Chand et al., 2010). While initially intended for wind energy problems, CgWind is a useful, general purpose wind engineering simulation tool. Currently under development at Lawrence Livermore National Laboratory, CgWind will be freely available for use by wind engineers, researchers and the general wind engineering community.

Verification and validation of CgWind are necessary precursors to its successful use as a wind engineering tool. Verification is the process whereby the algorithms and implementation of CgWind are shown to be correct. For complex mathematical models that are applied in complex geometries, verification is nontrivial. However, CgWind is implemented using the Overture software framework, which provides an extensive infrastructure for the verification of numerical techniques using the method of manufactured solutions (Chand and Henshaw, 2007). Rigorous verification is therefore incorporated into CgWind's development process. Once a numerical method is verified, validation of the mathematical model can begin. Validation of CgWind is accomplished by running the code on test problems that are relevant to wind engineering applications, and then comparing the numerical results with experimental data.

2 NUMERICAL APPROACH TO SOLVING THE NAVIER-STOKES EQUATIONS

CgWind solves the incompressible Navier-Stokes (INS) equations with a pressure-velocity formulation and a split-step method where the pressure is computed in a separate step. For a given domain Ω, with boundary $\partial\Omega$, the governing equations are

$$\begin{aligned} \mathbf{u}_t + (\mathbf{u}\cdot\nabla)\mathbf{u} + \nabla p - \nu\Delta\mathbf{u} - \mathbf{f} = 0, \qquad & t > 0, \quad \mathbf{x}\in\Omega \\ \Delta p + \nabla\mathbf{u} : \nabla\mathbf{u} - \alpha\nabla\cdot\mathbf{u} - \nabla\cdot\mathbf{f} = 0, \qquad & t > 0, \quad \mathbf{x}\in\Omega \end{aligned} \tag{1}$$

with appropriate initial conditions, $\mathbf{u}(\mathbf{x},0) = \mathbf{u}_I(\mathbf{x})$, and boundary conditions, $\mathcal{B}^F(\mathbf{u},p) = 0$. Here, $\mathbf{u}$ is the velocity, p is the pressure and ν is the kinematic viscosity. The term $\alpha\nabla\cdot\mathbf{u}$ in the pressure equation acts as a damping term on the divergence of the velocity. When buoyancy effects are important, an additional temperature equation is added following the Boussinesq approximation as described by Henshaw and Chand (Henshaw and Chand, 2009); buoyancy effects are ignored in this study. The use of LES turbulence models also adds an additional term to the equations. Previously, explicit second- and fourth-order accurate schemes have been developed to solve the equations on overlapping grids (Henshaw, 1994; Henshaw and Petersson, 2003). In this paper we describe the verification and validation of a new approach that combines high-order accurate compact schemes with implicit approximate factorization methods. This new method alleviates the small timestep restriction on high resolution grids imposed by the viscous timescale while preserving the efficiency of explicit finite difference methods.

CgWind also exploits the composite grid approach, which leverages the computational benefits of overlapping, structured grids to represent complex geometry (Chesshire and Henshaw, 1990). These grids are ideal for the high-order accurate compact discretizations used by CgWind as well as the matrix-free geometric multigrid algorithm that enables large-scale, high-resolution computations with realistic geometry (Henshaw, 2005). The memory and CPU performance advantages of high-order accurate methods on structured grids allows CgWind to perform simulations at spatial resolutions currently unobtainable by many other approaches. For example, CgWind's memory footprint for a three-dimensional computation can be as low as $1-2$GB per million grid points, depending on the number of overlapping grids and their topology. Consequently, high-resolution computations can be performed efficiently, even on modest workstations and clusters.

Currently, there are two subgrid-scale models in CgWind: a simple Smagorinsky style dissipation, and a high-order model that is more compatible with the resolution properties of CgWind's fourth-order spatial discretization. The high-order model relies on a hyperviscosity whose nonlinear coefficient is related to the local strain rate via the smallest scale estimates of Henshaw, Kreiss and Reyna (Henshaw et al., 1989). Other LES turbulence models are currently under development.

3 VERIFICATION

Verification is an essential step in the development of any computational modeling tool. Prior to using a code that approximates a given a set of equations, such as Equation 1, we must ensure that the numerical methods are implemented correctly and that their observed properties (stability and accuracy) match theoretical expectations. In the case of CgWind, this verification process tests both the basic numerical method and the implementation complexities related to the moving overlapping grid methods, the multigrid solver, and the boundary conditions.

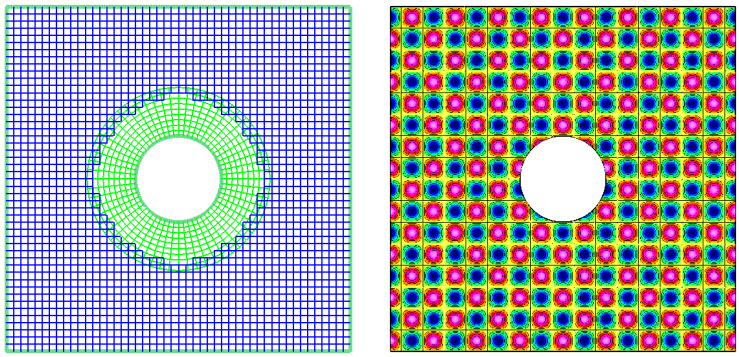

h_{max}	$\|e_p\|_\infty$	$\|e_u\|_\infty$	$\|e_v\|_\infty$	$\|\nabla \cdot \mathbf{u}\|_\infty$
6.13e-02	1.17e-02	4.35e-03	4.93e-03	9.36e-02
3.08e-02	7.16e-04	1.68e-04	1.72e-04	5.99e-03
1.54e-02	4.31e-05	1.14e-05	9.52e-06	4.45e-04
7.70e-03	2.91e-06	7.62e-07	6.67e-07	3.43e-05
rate	4.0	4.1	4.3	3.8

Figure 1: A two-dimensional overlapping grid (left) and "twilight-zone" (i.e., manufactured) solution (right). Errors and estimated convergence rates for a time dependent exact solution are listed in the table where h is grid spacing and $|e|_\infty$ denotes the maximum error norm. The timestep is reduced by a factor of one-quarter for each resolution so that the time errors scale at the same rate as the spatial errors.

While it is common to verify numerical methods using simple analytical solutions to the model equations, this approach is often hampered by the approximate nature of such solutions or reduced complexity (i.e., many are one-dimensional) needed to derive a closed form solution. In both cases, the performance of the numerical method cannot be verified in the presence of complex geometry and full dimensionality of realistic problems. In contrast, the method of twilight-zone (or manufactured) solutions provides a powerful technique for rigorously verifying the implementation of a numerical method in both simple and complex computational domains. In this approach, a solution to the governing equations is chosen as a function of space and time, and then the required forcing terms are derived to ensure the selected solution is exact. For example, if we choose

$$\mathbf{u}(\mathbf{x}, t) = \mathbf{c} \cos(\pi f_t t) \sin(\pi f_x x + s_x) \sin(\pi f_y y + s_y) \sin(\pi f_z z + s_z), \tag{2}$$

to be the solution, where $\mathbf{c}$ is a vector of coefficients, then the required forcing terms are derived by substituting this solution into the governing equations. The numerical method is then applied to the governing equations with the appropriate forcing, and the computed solution is compared to the exact solution. These verification tests ensure that the algorithms are implemented properly and that important properties of the method (e.g., order of accuracy, stability) are preserved. When implementing high-order accurate methods, for example, it is easy to introduce coding or algorithmic errors that produce solutions that are consistent but are not of the expected order of accuracy. Rigorous verification via the method of manufactured solutions is one of the few tools capable of detecting such errors.

Figure 1 illustrates a simple overlapping grid and a manufactured solution on this grid. The table in Figure 1 shows the estimated fourth-order convergence rates for CgWind's algorithms with a two-dimensional geometry and manufactured solution. Figure 2 shows pressure contours on cutting planes through a three-dimensional, time dependent manufactured solution for a cylinder in a box. This grid system consists of two grids: one Cartesian grid for the background, and one cylindrical grid for the cylinder. The accompanying table demonstrates the fourth-order accuracy of the numerical method for the full three-dimensional problem.

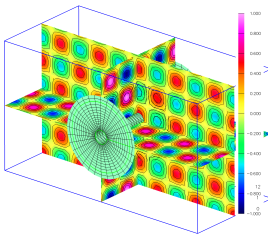

(a) grid and solution

h_{max}	$\|e_p\|_\infty$	$\|e_u\|_\infty$	$\|e_v\|_\infty$	$\|e_w\|_\infty$	$\|\nabla \cdot \mathbf{u}\|_\infty$
2.94e+00	5.10e-02	6.71e-02	3.56e-02	3.44e-02	1.52e-01
1.47e+00	3.62e-03	4.40e-03	2.19e-03	2.21e-03	2.28e-02
7.36e-01	2.62e-04	3.16e-04	1.44e-04	2.34e-04	1.34e-03
rate	3.8	3.9	4.0	3.6	3.4

(b) convergence rates

Figure 2: Grid, solution and convergence rates for a three-dimensional verification test.

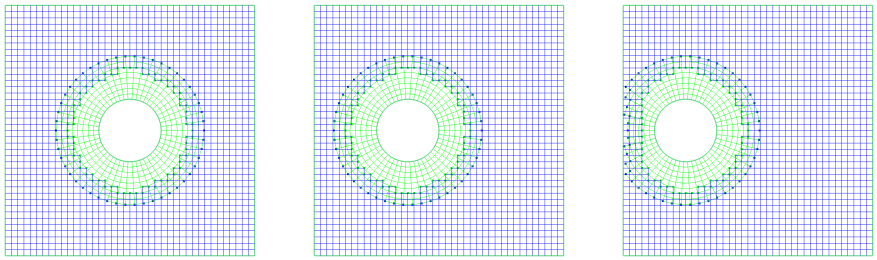

(a) $t = 0.0$ (b) $t = 0.5$ (c) $t = 1.0$

h_{max}	$\|e_p\|_\infty$	$\|e_u\|_\infty$	$\|e_v\|_\infty$	$\|\nabla \cdot \mathbf{u}\|_\infty$
6.84e-02	8.44e-02	1.80e-01	1.51e-01	1.80e+00
3.44e-02	1.72e-02	2.25e-02	2.61e-02	4.63e-01
1.72e-02	7.92e-03	5.49e-03	5.83e-03	1.54e-01
8.60e-03	2.69e-03	1.10e-03	1.39e-03	5.42e-02
rate	1.6	2.4	2.3	1.7

(d) convergence rates

Figure 3: Manufactured solution based convergence rate estimates for the translating cylinder test case. Currently second-order accurate boundary conditions are implemented for moving grids.

Moving grid algorithms present unique challenges in the context of verification. Boundary conditions that preserve both temporal and spatial accuracy are nontrivial to implement as are the algorithms that manage the dynamic grid generation and interpolation required with bodies in relative motion. Nevertheless, the method of manufactured solutions can be incorporated into the solver to test even this challenging case. While only second-order accurate moving grid boundary conditions are complete in CgWind, Figure 3 shows the second-order convergence rates for a translating cylinder and some of the intermediate grids generated during the computation. Note that this calculation can be performed in several ways. For example, the cylinder can remain stationary with the background grid "translating" via boundary conditions specifying the streaming velocity. Alternatively, the background grid can be stationary while the cylinder moves relative to it. Both cases are tested and yield similar results, with the moving cylinder results presented in the table.

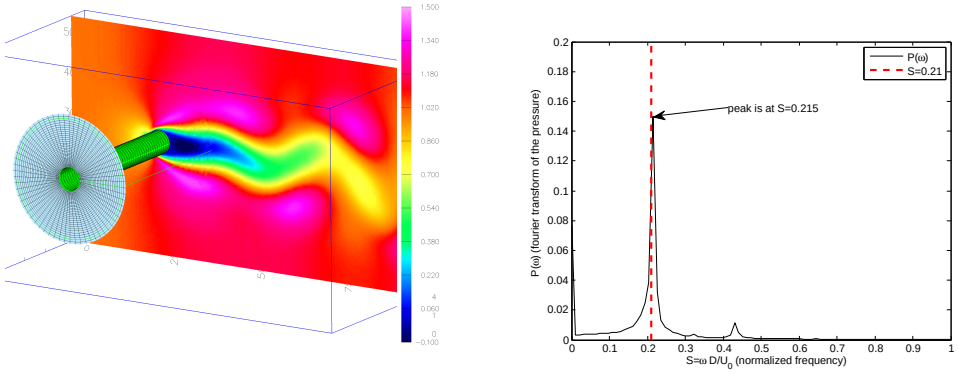

(a) cylinder grid and x-velocity, $t = 700s$

(b) Fourier transform of pressure signal vs nondimensional frequency (Strouhal number)

Figure 4: Flow at Reynolds number 1000 past a right circular cylinder. Note the dominant frequency matches the experimentally determined Strouhal number of 0.21, which is marked by the dashed vertical line.

4 VALIDATION

Once it is verified that a numerical model properly approximates the intended mathematical model, validation can then be performed to demonstrate the suitability of the mathematical model to represent the physical problem of interest. Generally, validation is performed by comparing the numerical results with corresponding experimental data for the problems of interest. In this case, CgWind is tested on three cases: transverse flow past a right circular cylinder, time dependent flow past an impulsively started rotating cylinder (Coutanceau and Menard, 1985), and flow at $Re = 12000$ past a steep hill (Ishihara et al., 1999). The first case tests the algorithm's ability to model resolvable (i.e., low Reynolds number) flows. The second case tests the second-order accurate moving grid algorithm. Finally, the third case is more directly relevant to wind engineering and exposes some current limitations of the code. Calculations of the first and third cases use the fourth-order accurate algorithm with the high-order LES model. The impulsively started cylinder problem requires no additional dissipation.

4.1 Three-dimensional flow past a circular cylinder

Figure 4 summarizes the results of a validation test consisting of a right circular cylinder placed in a freestream flow normal to the cylinder axis. The Reynolds number based on the streaming velocity and cylinder diameter is 1000. The inflow velocity is $U_0 = 1$; the outflow condition is the equation $p + \delta \frac{\partial p}{\partial n} = 0$, where δ is the length scale of the domain; and the remaining boundaries are slip walls.

The Strouhal number, $St = \frac{\omega D}{U_0}$, is computed and compared to the experimentally determined value of 0.21 (Schlichting, 1979). The flow is simulated to a nondimensional time of 700, and the pressure recorded at a point in the wake that is 8 diameters downstream of the cylinder. Figure 4 indicates that the dominant Fourier mode of the pressure signal matches the known shedding frequency.

Two composite grids (background and cylinder) with a total of approximately $400,000$ nodes are used to resolve the flow. The calculation required less than three hours of computation

time on six Xeon $2.2Ghz$ processors; approximately 1GB of memory is used. However, the overhead for each process in a parallel computation is approximately $80Mb$. Consequently, a single CPU computation requires less memory (about $600Mb$); however, such a computation also takes six times longer.

4.2 Two-dimensional impulsively started rotating cylinder

The Coutanceau and Menard investigation of an impulsively started rotating and translating cylinder provides an excellent validation case for time dependent calculations of bodies in relative motion (Coutanceau and Menard, 1985). This flow is characterized by two nondimensional parameters: the Reynolds number, $Re = \frac{U_0 D}{\nu} = 200$, where U_0 is the translational velocity, D is the cylinder diameter, and ν is the viscosity; and the rotation parameter, $\alpha = \frac{\omega D}{2U_0} = 0.5$, where ω is the angular velocity. The low Reynolds number of this flow facilitates adequate spatial resolution on relatively coarse grids, even with CgWind's second-order accurate moving grid discretization. For the comparisons shown, a cubic ramp function is used for the velocity that starts from $U_0 = \alpha = 0$ and reaches the steady-state values of $U_0 = 1$,$\alpha = 0.5$ at time 0.1. A two-dimensional configuration that uses two overlapping grids, similar to that shown in figure 1, is used. The two grids contain $368,530$ vertexes, which ensures adequate spatial resolution as determined by a grid resolution study.

Figure 5 shows the streamlines at a final nondimensional time of $t^* = \frac{tU_0}{2R} = 4$ as well as comparisons of the two velocity components as a function of distance behind the cylinder for several times. The calculations are performed twice: once with the cylinder rotating and translating (solid lines in the figure), and once with the cylinder rotating while the translation is imposed as boundary conditions on the background grid. As figure 5 indicates, both sets of results are in agreement with the experiment, especially considering the 5% estimated uncertainty in the experimental data.

Despite being two-dimensional and low Reynolds number, this computation is algorithmically complex. At each timestep the overlapping grids are adjusted for the rigid body motion, interpolation points are recomputed, and newly exposed points are interpolated.Nevertheless, the calculations are run with $368,530$ grid points, consume 177MB, and take 747 steps in less than one hour on a single CPU (Intel Xeon 2.2Ghz).

4.3 Three-dimensional steep hill

Ishihara et al. and Hibi et al. conducted experiments of flow past a model hill with varying surface roughnesses that provide data for validation purposes (Ishihara et al., 1999; Meng and Hibi, 1998). The hill is defined by the profile $z(r) = Hcos^2(\frac{\pi r}{2L})$ for $r \leq L$; $z(r) = 0$ for $r > L$; where $r = \sqrt{x^2 + y^2}$, H is the height of the hill $(40mm)$ and $2L$ is the hill's width $(200mm)$. The Reynolds number based on H is approximately 12000. The domain for our calculations consists of a box, centered on the hill, of dimensions $28H$x$25H$x$6H$ in the x, y and z axes, respectively. Inflow velocity is given by the power law boundary layer profile provided by Ishihara et al., while the hill and lower wall have no-slip (zero velocity) boundaries. The remaining computational boundaries are outflows with a mixed condition on the pressure given by the equation $p + \delta \frac{\partial p}{\partial n} = 0$, where δ is a length scale for each direction.

Figure 6 depicts the results from a calculation with $4x10^6$ grid points on 128 processors. While qualitatively "correct" in many respects, the results do not match the experimental data in the wake. However, the numerical results should be studied with the caveat that wall models are

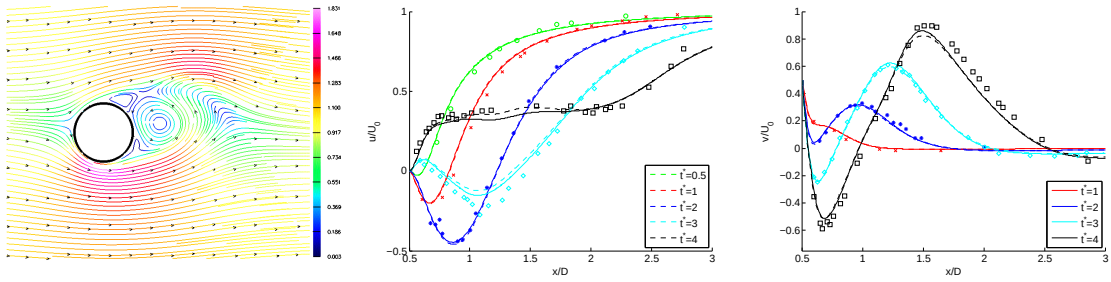

(a) streamlines at t^*=4 (b) x-velocity comparison (c) y-velocity comparison

Figure 5: Streamlines and comparisons with experimental data for the $Re = 200$ flow near an impulsively started rotating and translating cylinder. Solid curves show results for both rotation and translation of the cylinder; dashed lines depict the rotating cylinder with the freestream imposed via boundary conditions; symbols are the experimental data. These results are sensitive to the startup time scale.

not implemented. Consequently, these comparisons are shown for ill resolved no-slip boundary conditions. The wall grid spacing was eighteen times larger than the experimentally estimated roughness scale. Nevertheless, this spacing results in very fine grids near the boundary that, even with the implicit algorithm, required small timesteps and 56 hours of computer time.

We hope to improve on these results by implementing wall models that accurately account for surface roughness. In retrospect, it was optimistic to use this case as an initial validation study due to the aerodynamically rough nature of the flow. A wall model would also obviate the need for such fine grid spacing, thereby allowing quicker turn around on such problems. This case also highlights optimization scaling issues within our algorithms that need to be addressed.

5 STATUS AND FUTURE WORK

CgWind is under active development. The verification and initial validation results suggest that the core numerical algorithms are functioning as expected. However, validation tests, such as the steep hill, indicate the need for more work in phenomenological modeling of relevance to wind engineering applications as well as further verification. These verification and validation processes are only the beginning of a continuous effort to ensure that CgWind provides accurate and useful results. We expect to release the current version of the solver in the summer of 2011. An older version, along with documentation, (`cgIns`) can be found at `http://computation.llnl.gov/casc/Overture/`.

6 ACKNOWLEDGMENTS

The authors wish to thank Bill Henshaw for his contributions to the code, algorithms and theory that form the basis of this work. This work was performed under the auspices of the U.S. Department of Energy (DOE) by Lawrence Livermore National Laboratory under Contract DE-AC52-07NA27344, by Laboratory Research and Development funding and by DOE contracts from the ASCR Applied Math Program. LLNL-CONF-483351

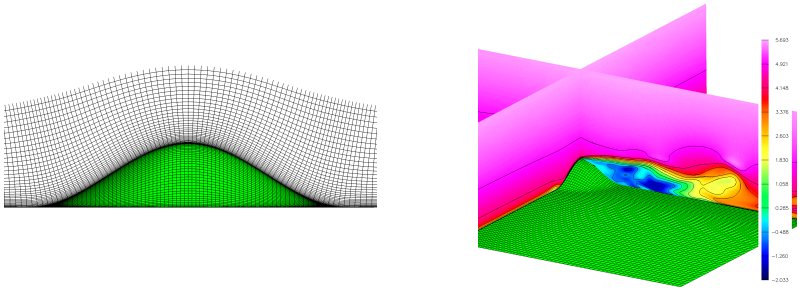

(a) grid near the hill (b) x-velocity contours

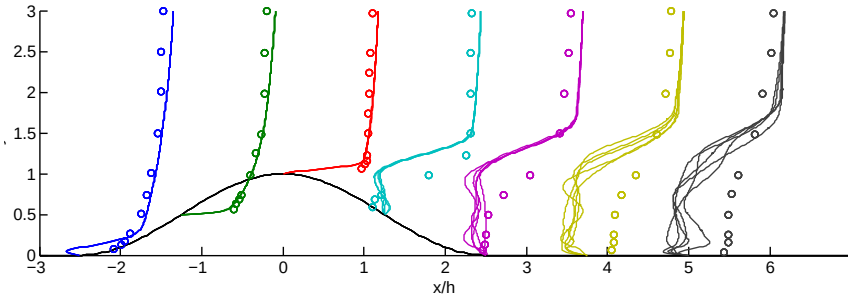

(c) instantaneous u/U_0 (curves) and experimental values (circles)

Figure 6: Grid, x-velocity contours and experimental comparison for the $Re = 12000$ flow past a steep hill. Note that no wall model is used to account for surface roughness, which may be a source of the poor agreement.

REFERENCES

Kyle K. Chand and William D. Henshaw. Overture. Technical Report http://www.llnl.gov/CASC/Overture, Lawrence Livermore National Laboratory, 2007.

Kyle K. Chand, William D. Henshaw, Katherine A. Lundquist, and Michael A. Singer. Cgwind: A high-order accurate simulation tool for wind turbines and wind farms. In *The Fifth International Symposium on Computational Wind Engineering*, 2010.

G. S. Chesshire and W. D. Henshaw. Composite overlapping meshes for the solution of partial differential equations. *J. Comput. Phys.*, 90(1):1–64, 1990.

Madeleine Coutanceau and Christian Menard. Influence of rotation on the near-wake development behind and impulsively started circular cylinder. *Journal of Fluid Mechanics*, 158:399–446, 1985.

William D. Henshaw. A fourth-order accurate method for the incompressible Navier-Stokes equations on overlapping grids. *J. Comput. Phys.*, 113(1):13–25, July 1994.

William D. Henshaw. On multigrid for overlapping grids. *SIAM Journal on Scientific Computing*, 26(5):1547–1572, 2005.

William D. Henshaw and Kyle K. Chand. A composite grid solver for conjugate heat transfer in fluid-structure systems. *J. Comput. Phys.*, 228:3708–3741, 2009.

William D. Henshaw and N. Anders Petersson. A split-step scheme for the incompressible Navier-Stokes equations. In M.M. Hafez, editor, *Numerical Simulation of Incompressible Flows*, pages 108–125. World Scientific, 2003.

William D. Henshaw, H.-O. Kreiss, and L. G. M. Reyna. On the smallest scale for the incompressible Navier-Stokes equations. *Theoretical and Computational Fluid Dynamics*, 1:65–95, 1989.

Takeshi Ishihara, Kazuki Hibi, and Susumu Oikawa. A wind tunnel study of turbulent flow over a three-dimensional steep hill. *Journal of Wind Engineering and Industrial Aerodynamics*, 83:95–107, 1999.

Yan Meng and Kazuki Hibi. An experimental study of turbulent boundary layer over steep hlls. In *15th National Symposium on Wind Engineering*, pages 61–66, 1998.

H. Schlichting. *Boundary-Layer Theory*. McGraw-Hill, New York, 1979. Seventh Edition.